ARCTIC RESPONSE TECHNOLOGY
OIL SPILL PREPAREDNESS

July, 2017

John H Bradford, HP Marshall, Bob Hay, Boise State University
Nathan Lamie, Cold Regions Research and Engineering Lab

CONTINUED DEVELOPMENT OF AN FMCW RADAR SYSTEM FOR AIRBORNE DETECTION OF OIL SPILLS UNDER AND IN ARCTIC SEA ICE

SUMMARY

A controlled crude oil spill was conducted under ~30 cm of cold ice grown in a 4 x 4 x 1 m test basin. The ice sheet was comparable in salinity and surface temperature to mid-winter ice in the Beaufort Sea. One barrel of Alaskan crude was injected into a 2 x 2 m recessed area in the center of the basin that was created by removing the first 5 cm of ice growth. This resulted in an approximately 5 cm thick oil layer at the base of the ice. The FMCW radar, mounted 1.7m above the ice surface, produced a clear image of the ice surface and of the base of the ice. Introduction of the 5 cm oil layer resulted in an amplitude increase of 30% which is well above the noise level and approximately consistent with modeling results. One complication was that oil was observed migrating through the ice sheet just 2 hrs after injection. This rapid migration likely resulted in a decreased radar response that occurred sooner than expected. This condition differs from natural ice growth where oil spilled under cold ice has been observed to form a discrete layer that persists for months with little upward migration, and we would expect the strong radar response to persist as long as the discrete oil layer remains intact. Ice growth beneath the oil was monitored for 38 hrs after the spill, and changes in radar response during this period are consistent with modeling results, specifically predictable amplitude differences and peak broadening are associated with the growing layer of encapsulating ice. This basin test represents the first confirmed detection of oil under ice with the FMCW radar and represents substantial progress in efforts to develop a purpose built radar for deployment from an airborne platform.

TABLE OF CONTENTS

LIST OF FIGURES

1 INTRODUCTION AND BACKGROUND

The lack of any practical operational remote sensing system to detect oil in ice was identified as a priority research gap in Dickins (2004). The need for proven and reliable systems to detect oil trapped in a range of ice conditions remains at the forefront of continued efforts to advance Arctic spill response capabilities.

In previous phases of this project, our research team has made significant progress in the development of oil-in-ice and oil-under-snow detection utilizing off-the-shelf ground-penetrating radar (GPR). Through a series of related projects involving numerical modeling, laboratory trials, and field tests in a range of ice conditions, we have demonstrated that ground-based commercially available GPR systems operating in the 500 MHz to 1 GHz range are effective tools to deal with the problem of detecting oil in, on and under ice. The same systems in a low-altitude airborne mode are capable of reliably detecting oil on the ice surface buried under snow.

From the results of the initial airborne tests with the commercial pulsed radar, it was determined that to reliably detect spills beneath the ice from an airborne platform, it would be necessary to develop a new radar system that produced more power and had improved directionality to minimize scattering noise from the aircraft. The radar system selected was a frequency-modulated continuous wave (FMCW) type radar with a highly directional horn antenna.

Following tests with the first prototype of the new airborne radar system at CRREL in early 2011, the team carried out a series of hardware improvements and developed a second prototype. The aim was to achieve an unambiguous detection of oil under ice that would justify further testing and airborne trials.

The second prototype was tested at CRREL in February 2012 with crude oil spilled under 45 cm of sea ice grown in the same outdoor tank as the previous year. Unfortunately, in that test, the internal ice temperature was too warm to allow sufficient penetration of radar energy to the ice/oil/water interface to demonstrate conclusive detection. In spite of this setback, valuable data gained from analyzing the 2012 CRREL test data guided further hardware enhancements, incorporated in a third FMCW prototype designed and built in the fall of 2012.

Prototype 3 (P3) achieved its design objectives, including a significant improvement in signal to noise ratio over the available commercial impulse GPR, increased scan rate and ability to measure phase changes. In previous field tests in Norway 2006, phase anomalies were an important attribute in detecting oil under ice.

In the 2015 JIP project, data were collected throughout the entire 3-month experiment. The majority of measurements were corrupted by noise in the system, electromagnetic noise in the facility, and connection problems. We suspect that some of the system noise problems were related to the antenna modifications which were required to make this system viable for helicopter operations. This was the first long-term test of this kind with this prototype. While this prototype showed some promising results, it was determined that additional improvements were required to make both the hardware and control software robust.

The limited data processed from the moving FMCW suspended above the ice in 2015 indicated that the system was able to detect oil trapped within the ice from above. Additionally, a second fixed radar appeared to show a clear response to oil injected under the ice, however the dataset was too limited to make an unambiguous interpretation.

The key objective of current project was to upgrade and test the FMCW prototype under cold, and consistent ice conditions. Specifically, the project had four primary goals:

1. Upgrade the FMCW hardware to overcome the reliability issues that affected the 2015 tests.
2. Conduct tests of the improved FMCW system at CRREL over a test ice sheet prepared in advance, with ice thickness and dimensions determined jointly by CRREL and Boise State staff. Note that CRREL provided all necessary facilities including an overhead attachment point and necessary ice documentation (subject of a separate RFP).
3. Train CRREL technician(s) in the use of the FMCW such that they could obtain and log the necessary data over an encapsulated oil layer with data acquisition occurring in the days following the initial oil spill.
4. Process and analyze the data in a form that becomes part of a final test report, including comparisons of results with model predictions and recommendations for a future test program.

The target ice conditions were cold ice (surface temperature < -10 C), 30 cm ice thickness, and 5 – 7 ppt internal salinity which would be similar to mid-winter ice in the Beaufort Sea. Alaska North Slope crude oil would be injected under the ice to create an oil layer 3 to 5 cm thick. A first ice sheet grown for radar testing in January 2017 did not meet salinity specifications. Approximately 30 cm of ice was grown rapidly at -25 C. The rapid ice growth did not allow for efficient expulsion of salt from the ice matrix and the resulting salinity profile was significantly higher than would likely be observed in nature with salinities of ~10 ppt in the core of the ice sheet for the trial vs ~5 ppt for a natural ice sheet (Figure 1). The result of a high salinity profile is increased radar attenuation. As the modeling simulation shown in Figure 2 illustrates, a more realistic salinity profile would result in roughly 5 times more energy in the base-of-ice return. With the resulting high electrical conductivity in the ice, the radar failed to produce an interpretable signal from the base of the ice sheet. A new ice sheet was grown for a second trial from June 5-13, 2017. The second ice sheet met design specifications for temperature and salinity. The radar performed well during the injection of 5 cm oil and for 38 hours following the injection. The ice surface, base of ice, and a response associated with the input of oil were observed.

Figure 1 Measured salinities from a radar test conducted at Prudhoe Bay in 2005.

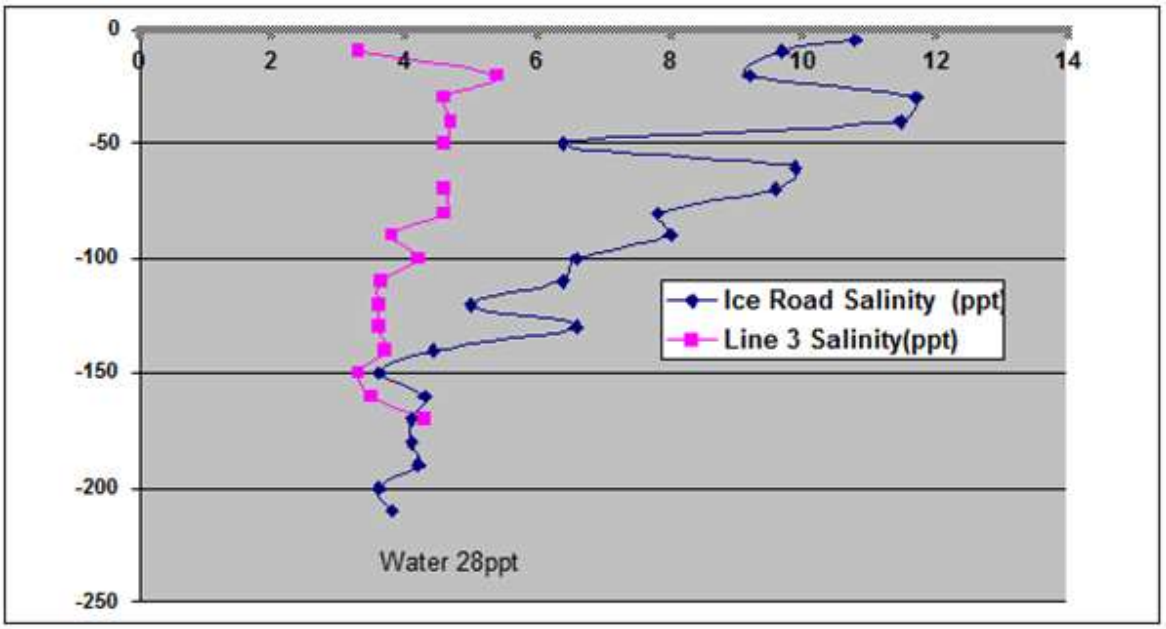

Salinities on the ice road (blue) are artificially high and similar to the salinities produced in the CRREL ice sheet during the January 2017 test. Radar signal could not penetrate the ice road. Salinities in the natural fast ice (pink) are roughly half that of the ice road through the central part of the ice sheet. Strong radar returns were observed from the base of the natural ice. (Figure courtesy of DF Dickins)

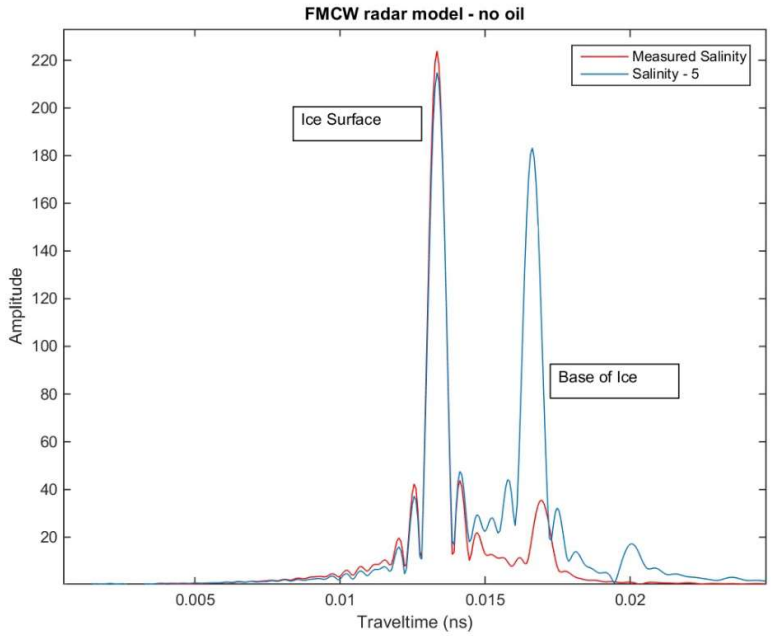

Figure 2 Modeled radar returns with the measured ice salinity during the January 2017 test (red), and with an ice salinity closer to the natural ice profile of Figure 1.

We expect a roughly 5 times greater amplitude return in the more natural ice salinity profile.

2 RADAR SYSTEM MODIFICATIONS

In order to improve radar performance over the 2015 JIP tests conducted at CRREL, a number of radar modifications were implemented. Initial improvements included: 1) an external broadband amplifier to boost transmitted signal, and 2) a new generation antenna that is lighter and cheaper making it feasible to build and implement a practical, polarimetric system. These implementations were tested during the January 2017 trial. It was found that the old antennas (modified horn antennas from P1) had superior performance to the new generation antenna and the P1 antennas were utilized for all subsequent tests. During the January test, the radar operated continuously for several days, but then failed. The external amplifier was the component suspected to have caused the failure so the system electronics were redesigned for the June, 2017 tests. The goals for the redesign were to improve the stability at low frequencies and to reduce the noise floor, thereby eliminating the need for the external amplifier. The details of the electronics changes are given in Appendix A. In addition, the same modifications were made to the P2 system, which provided duplicate systems with the most up to date specifications. This provided a backup system for the June test and in the future will provide flexibility in radar deployments.

Despite the problems with the January basin trial, several tests were performed that led to improved radar performance. Specifically, the radar antenna separation was optimized to maximize the primary reflection energy while minimizing the multiple reflections from the ice surface, and several measurements were made with a network analyzer which will aid in future system design.

3 JUNE BASIN TRIAL

3.1 Ice sheet preparation

The ice sheet was grown in a 4 x 4 x 1 m tank. Initial ice growth was carried out with an air temperature of -10 °C for slow growth in order to allow adequate time for brine expulsion from the ice matrix. After 5 cm of ice growth, a 2 x 2 m section of ice was removed from the center of the tank in order to provide a recess to capture the injected oil. Four days prior the planned oil injection, the temperature was decreased to -25 °C to ensure a cold ice sheet and to reach the target ice thickness of 30 cm (Figure 3). Injection of the oil required that the bay doors remain open for approximately 3 hrs which significantly raised the air temperature in the room, but warmed only the upper 15 cm of ice. At 1:30 pm on June 6, a full barrel of Alaskan crude was gravity fed through injection ports underneath the ice to create a 5 cm thick layer of oil at the base of the sheet. At approximately 2:00 p.m. the bay doors were closed and by 2:51 p.m. the temperature profile had recovered to the pre-injection values.

Figure 3 Photo of the prepared ice sheet prior to oil injection.

The 2 x 2 m recessed area is clearly evident and the oil injection ports can be seen at the top of the photo.

3.2 Ice conditions at time of oil injection

Ice conditions at the time of the oil injection met the design specifications and were close to mid winter temperature and salinity expected with thick fast ice in natural conditions (Figure 4). The ice thickness in the center of the tank was ~30 cm as estimated from radar traveltime

measurements. Coring at the end of ice growth showed that the ice thickness was 25 – 30 cm at the time of oil injection.

As shown in Figure 5, the ice temperature at the surface was just above -14 °C just prior to the injection on June 6. An inevitable temperature increase occurred during the oil injection because it was required that the bay doors remain open for approximately 3 hrs. During this period, the air temperature just above the ice rose to -6 °C and the ice surface temperature rose to -8 °C. Below 15cm ice depth, the temperature increase was negligible. The increase in surface temperature of the ice was sufficient to effect radar performance. A slight increase in surface reflection amplitude occurred due to the increase in electrical impedance at warmer temperatures. A decrease in base of ice reflection amplitude occurred due to increased signal attenuation with warmer ice near the surface. Despite these changes, the base of ice reflection could still be clearly seen throughout the experiment and measurable changes were observed during the oil injection (see section 3.4). The greater difficulty related to the temperature increase was the build up of condensation (Figure 6) on the radar antennas which likely resulted in a significant increase in system noise. Additionally, some minor temperature related shifts in the radar signal were observed due to temperature changes. At the time of oil injection the radar had equilibrated to temperature.

Post experiment coring showed ice salinities in the range of 5-6 ppt in the central core of the ice sheet with one sample below 3 ppt (Figure 4). Thus, the majority of the ice sheet met the design parameter of 5-7 ppt and provided realistic test conditions for the radar.

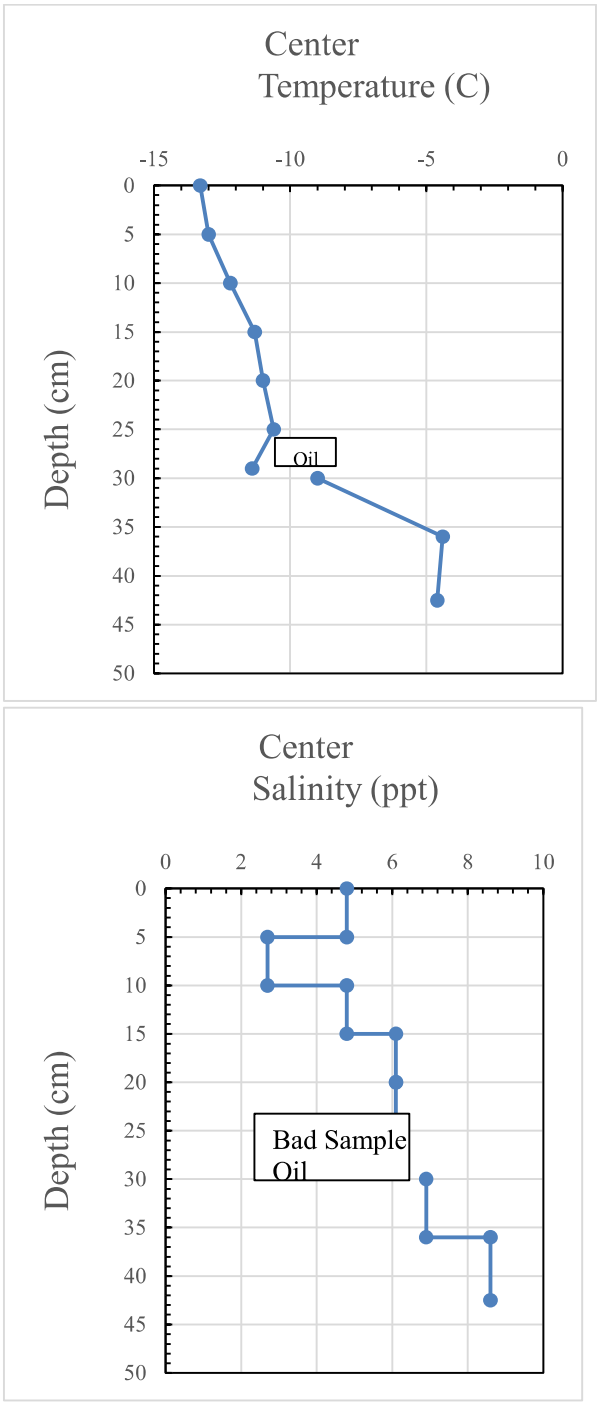

Figure 4 Ice temperature and salinity on June 13 at the completion of the test.

The temperature profile and salinities are comparable to values observed in thick, late winter ice in Prudhoe Bay (Figure 1) and provide a good test for radar performance in natural conditions.

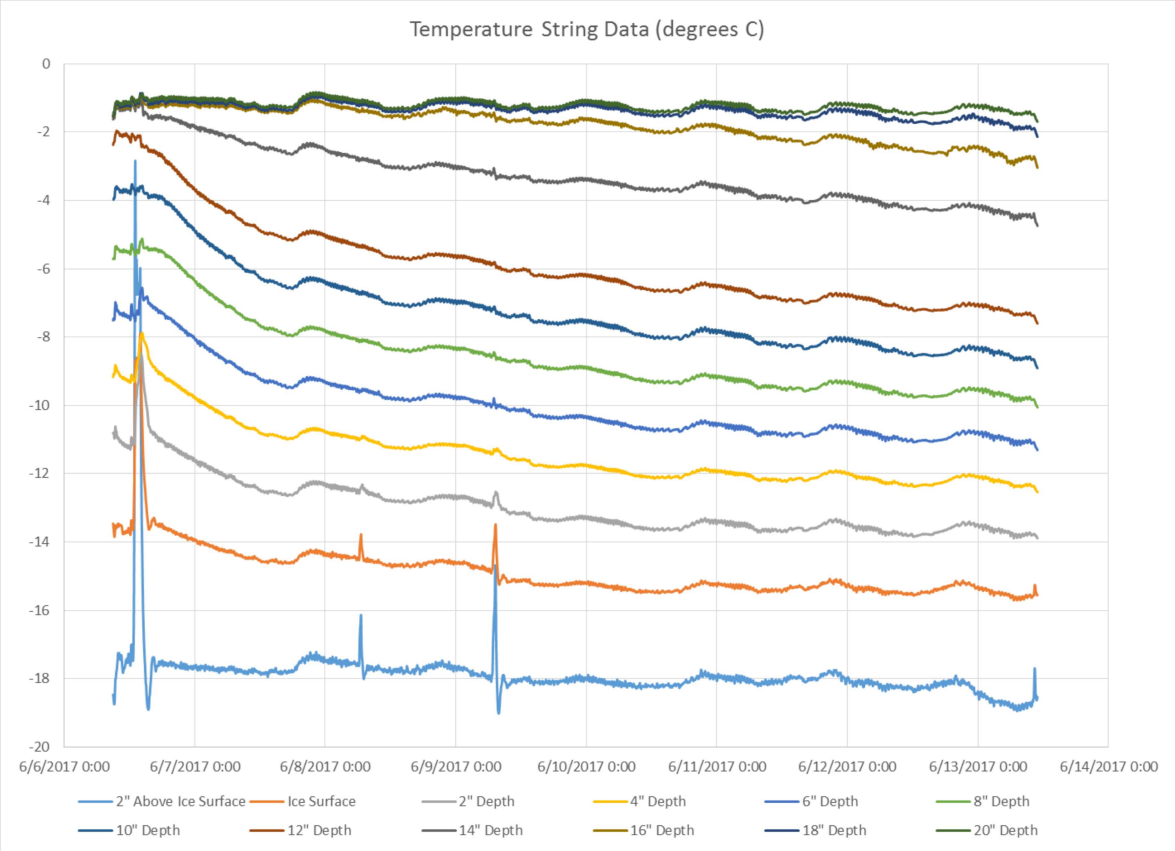

Figure 5 Ice temperature as a function of time and depth with the measurements beginning on the second day of radar testing and just prior to the oil spill.

The temperature spike observed at mid day on June 6 was the result of the bay doors being opened for approximately 3 hrs during the oil injection. Another spike on June 8 is associated with a power outage at which time normal operation of the radar ceased.

Figure 6 Condensation in the lab as the temperature warmed to outside air temperature while the bay doors were open.

3.3 Pulsed radar control measurements

As a control for the airborne FMCW radar trial, surface coupled impulse radar measurements were made using CRREL's GSSI SIR 3000 system with 900 MHz antennas. This system produces a radar pulse with a bandwidth comparable to the theoretical bandwidth of the FMCW radar (500 – 2000 MHz). Two types of measurements were made.

First, the GSSI radar antenna was placed in the center of the test cell and rotated through 360 degrees about the center point. This measurement was made to determine if azimuthal anisotropy was present in the ice and if so, the optimal orientation of the electrical field polarization. This measurement showed clear azimuthal anisotropy of the ice as indicated by a cyclic increase and decrease in reflection amplitude as the antennas were rotated (Figure 7). The same pattern of anisotropy was observed before and after oil injection. Amplitude variation of a reflector located at 2 ns traveltime (~15 cm depth) indicates a preferred brine pocket orientation that is aligned with the tank axis along the NE-SW direction. A reflection at 4 ns (~28 cm depth) is from the base of the ice. This reflection has a maximum amplitude that is about 30 degrees out of phase with the shallow reflection indicating that between 15 cm and 30 cm there is a rotation of ice crystal axes relative to the surficial ice. This may be related to an alteration of convection currents after a section of ice was removed to create a 2 x 2 m recessed area in the center of the tank to contain the oil spill. Based on these data we chose to orient the FMCW antenna with a field polarization orientation of 90 degrees (SE- NW) relative to the long axis of the lab.

The second type of measurement made with the pulsed radar was a standard profile through the center of the tank, before and after oil injection. These radar profiles show a clear increase in amplitude (Figures 8 and 9) and phase (Figure 10) associated with the placement of the 5 cm thick oil layer.

The results of the data collected with the pulsed layer provide a baseline for comparison with the FMCW results.

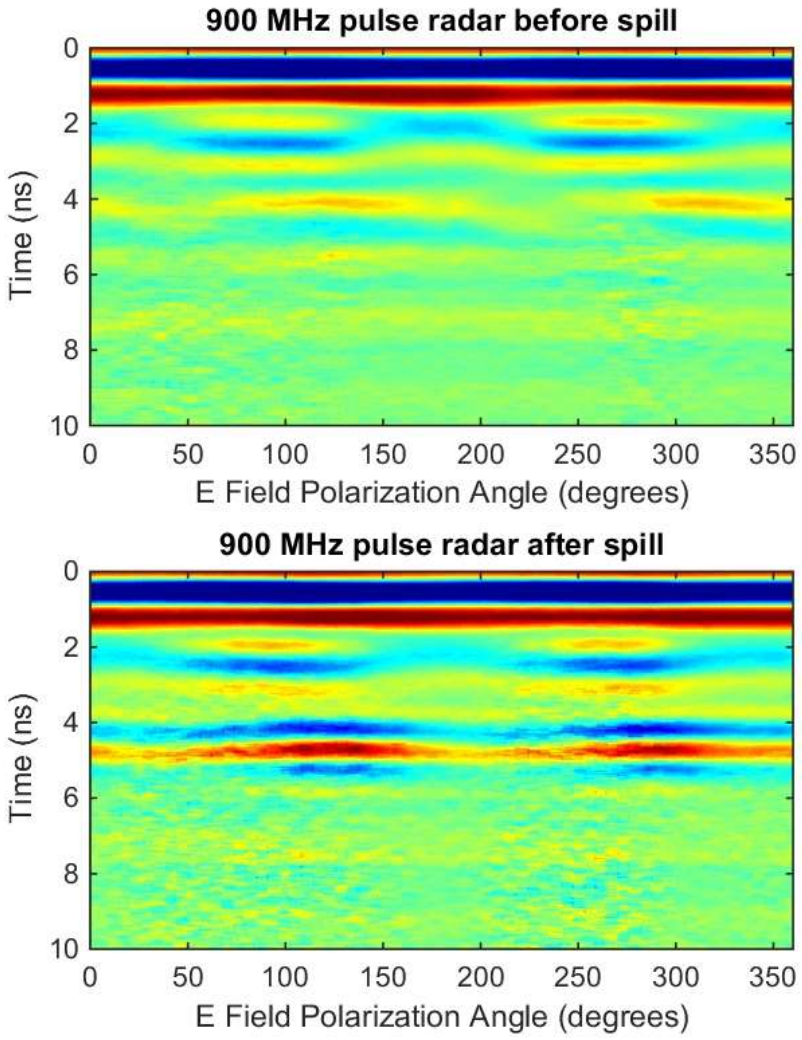

Figure 7 Radar profiles designed to test for azimuthal anisotropy by rotating the antenna through 360 degrees.

Cyclic increase in amplitude indicates a preferred orientation of brine pockets in the ice. High amplitudes are perpendicular to brine pocket orientation.

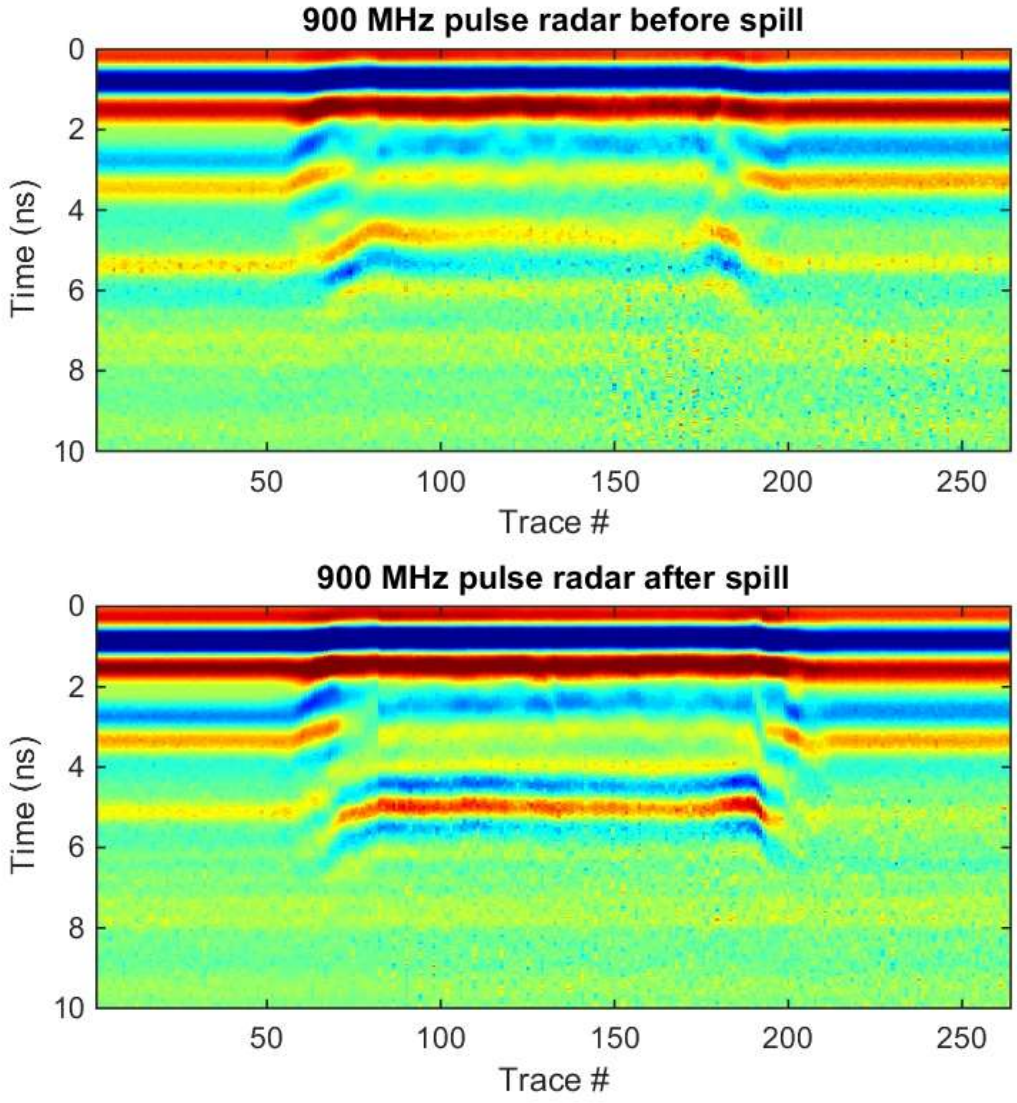

Figure 8 Pulse radar profiles through the center of the tank before and after oil injection.

The base of ice is at 4 to 5 ns. These profiles clearly show the raised containment area in the center of the tank and clear amplitude and phase anomalies associated with the 5 cm thick oil layer.

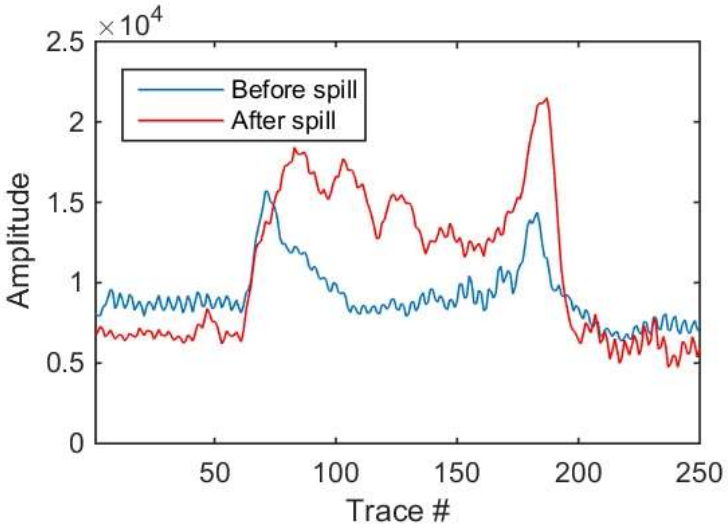

Figure 9 Instantaneous amplitude from the base of ice reflections taken from the data shown in Figure 8.

There is approximately a 50% increase in amplitude associated with the 5 cm oil layer.

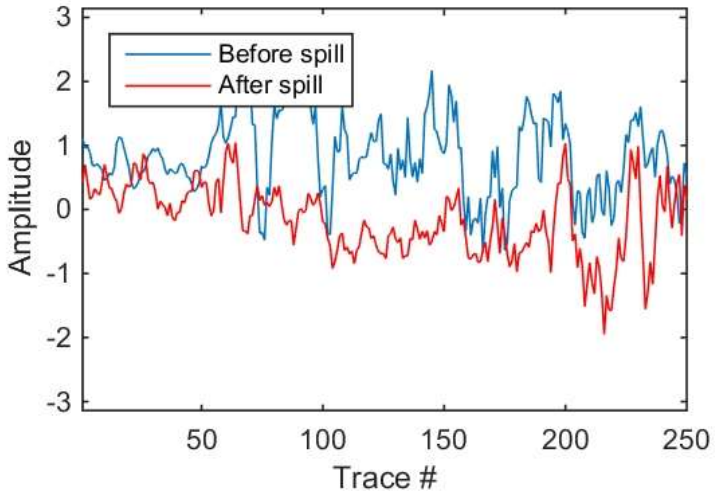

Figure 10 Phase calculated from the data shown in Figure 8.

Although a noisier signal, the phase rotation in the pulsed radar associated with the oil injection is evident.

3.4 FMCW Radar Results

The first set of measurements on June 5, one day prior to the oil spill, consisted of raising and lowering the FMCW radar antenna from the ice surface to ensure that the surface reflection was correctly identified. Then, after conducting pulsed radar tests to determine the optimal polarization direction as described in section 3.3, the FMCW antennas were mounted to the overhead gurney with the phase center 1.7 m above the ice surface – this was the maximum possible height (Figure 11). The radar was then configured to collect a trace every minute and was started 3 hrs prior to the oil spill. Ninety nine minutes after the radar started, the bay doors were opened and the room warmed substantially approaching the outside air temperature. This temperature increase resulted in a large amount of condensation (Figure 6). The radar required approximately 60 minutes to equilibrate to the temperature increase and the system noise increased significantly, likely due to condensation on the radar antennas. Throughout these changes the ice surface and base of ice reflection were clearly observed. The oil injection began at approximately 1:30 pm on June 6 and was completed by 1:58 pm. A full barrel of Alaskan crude was injected into the 2 x 2 m, 5 cm deep recess at the base of the ice to create an oil layer that was approximately 5 cm thick.

The base of ice reflection amplitude increased gradually over the ~30 minute oil injection, then gradually decreased toward the base value (Figures 12 and 13). The maximum amplitude increase is 30% higher than the base value and this amount of increase is consistent with model predictions (See section 4.0). A small but measurable phase rotation correlates with the amplitude increase (Figure 13). The maximum amplitude increase is coincident with the completion of oil injection, roughly 30 minutes after it began. The gradual increase in amplitude is consistent with the oil layer growing from 0 cm at the beginning of injection to a maximum thickness of 5 cm. Thus, the radar captured a range of oil layer thickness measurements between 0 and 5 cm, although there were not independent control measurements during this time. After reaching the maximum value the amplitude gradually decreased, nearing the base value 45 minutes after the oil injection ceased.

The amplitude increase is consistent with modeling, but the subsequent amplitude decrease is not. While this is not fully understood, there are two possible explanations. First, roughly 75 minutes after the oil injection began, oil was observed coming to the surface in the center of the tank. This was not expected for ice at these temperatures. Because this ice was grown entirely under quiescent conditions, it lacked a layer of frazil ice at the surface and had columnar crystals throughout. It is possible that this resulted in continuous brine channels through which the oil could migrate rapidly to the surface. Since the oil migrated rapidly into the ice, the sharp upper boundary assumed in the radar model quickly became a diffuse boundary altering the interference pattern and resulting in a lower amplitude radar response. This condition would not likely occur in a natural spill under cold mid winter ice. In controlled field spills under natural ice, a discrete oil layer has been observed to persist for months with little upward migration (Dickins and Buist, 1981; NORCOR, 1975). The rapid migration of oil during the June basin test coupled with similar occurrences in earlier basin tests (Dickins et al., 2005) suggests a fundamental difference in the crystal structure between basin grown ice and natural which results in increased

permeability of the basin grown ice. It is expected that the corresponding strong radar response would persist as long as the discrete oil layer was present which in natural sea ice would likely be for long periods after a spill.

The second possible explanation is one of resolution. The bandwidth of the FMCW radar system is 1500 MHz. This should result in a theoretical resolution of 4 cm at ice velocity. The effective observed resolution was on the order of 15 – 20 cm, which correlates to an effective bandwidth of around 500 MHz. The reason for the decrease in the effective resolution relative to the theoretical resolution is not yet understood, but likely is due to a complex interaction between the modified horn antennas, the antenna separation, and a non-point source. This decreased effective resolution may also explain the discrepancy between the response of the pulsed radar and the FMCW radar.

Approximately 75 minutes after the spill began the FMCW radar was stopped in order to take the suite of surface coupled pulsed radar measurements. Then 2hrs after the spill began, the FMCW was restarted for long term monitoring of the growth of an encapsulating ice layer beneath the oil. After 38 hrs a power outage stopped radar acquisition. CRREL personnel restarted the radar the following morning and it continued to run for the remaining 5 days, however it was not collecting data – it is likely that one of the steps in the restart was missed. Nevertheless the 38 hrs of data collected during encapsulation provide useful information.

The amplitude and phase of the system remained consistent and stable throughout the 38 hr measurement period. During this time, temperature measurements indicated that approximately 4 cm of encapsulating ice (Figure 4) grew beneath the oil. The ice surface reflection amplitude remained constant, while the base of ice amplitude varied systematically (Figures 14 and 15). These systematic changes in amplitude from the base of ice are consistent with the changing composite interference pattern from the base of the ice as the distance between the base-of-oil and base-of-ice interfaces changes. During this period, the peak width of the base of ice reflection increased as the composite reflection arises from a broader zone of reflectivity. Additionally, there is a shift to greater traveltime indicating the increasing ice thickness. The apparent increase in ice thickness is approximately 2 cm, rather than the 4 cm estimated from temperature measurements. This is consistent with modeling (see section 4.0) and occurs because the base-of-ice and oil reflections are not well resolved.

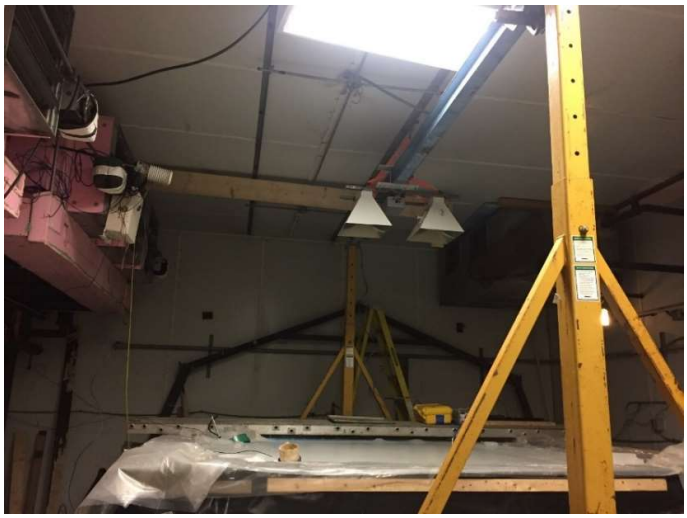

Figure 11 Photo of the FMCW radar mount.

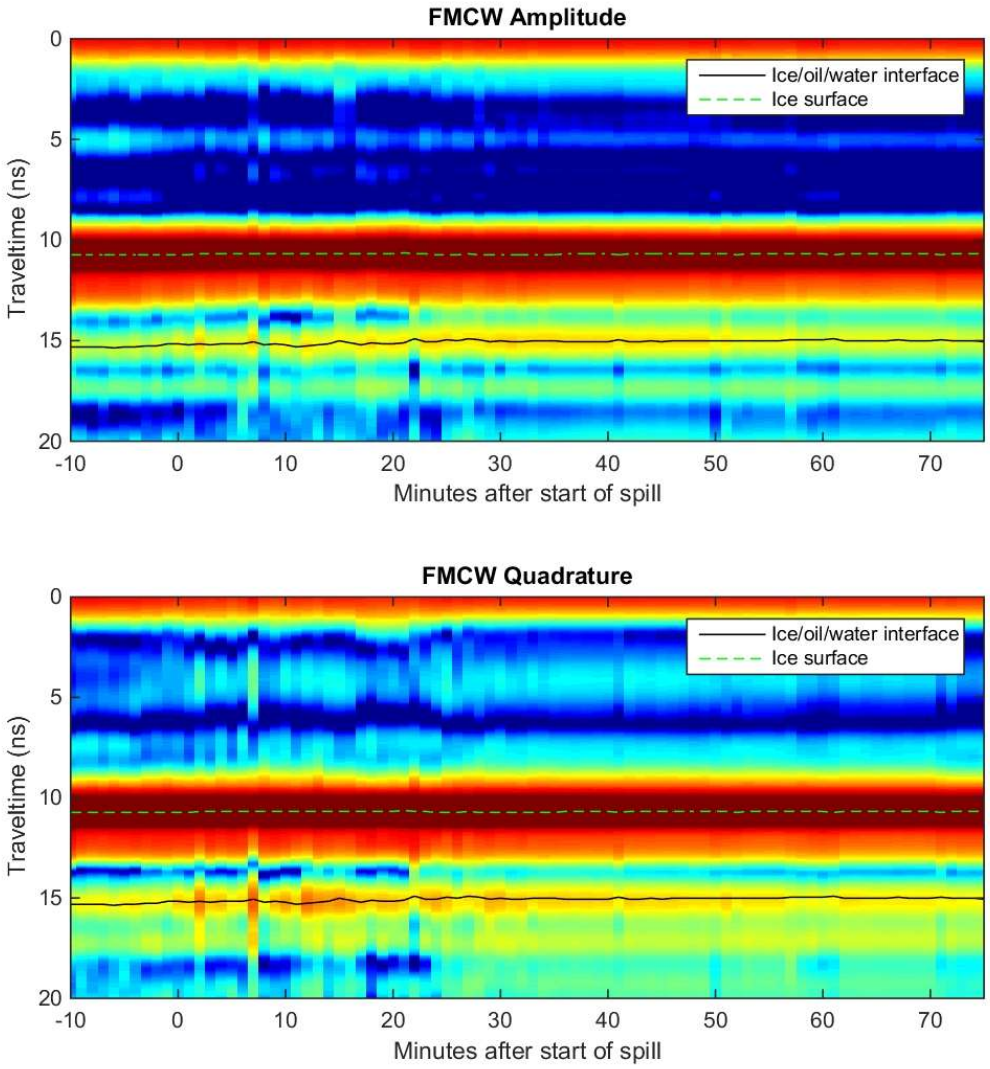

Figure 12 FMCW amplitude and out-of-phase (quadrature) component during and for a brief time after the injection.

The radar is mounted 1.7 m above the ice at the center of the spill area. Reflection amplitude from the ice surface remains stable and constant, while reflection amplitude and quadrature from the base increase gradually until the spill volume reaches its maximum value 30 minutes after the spill began. After this time the amplitude slowly decreases. Note the lower resolution relative to pulsed radar (Figure 8).

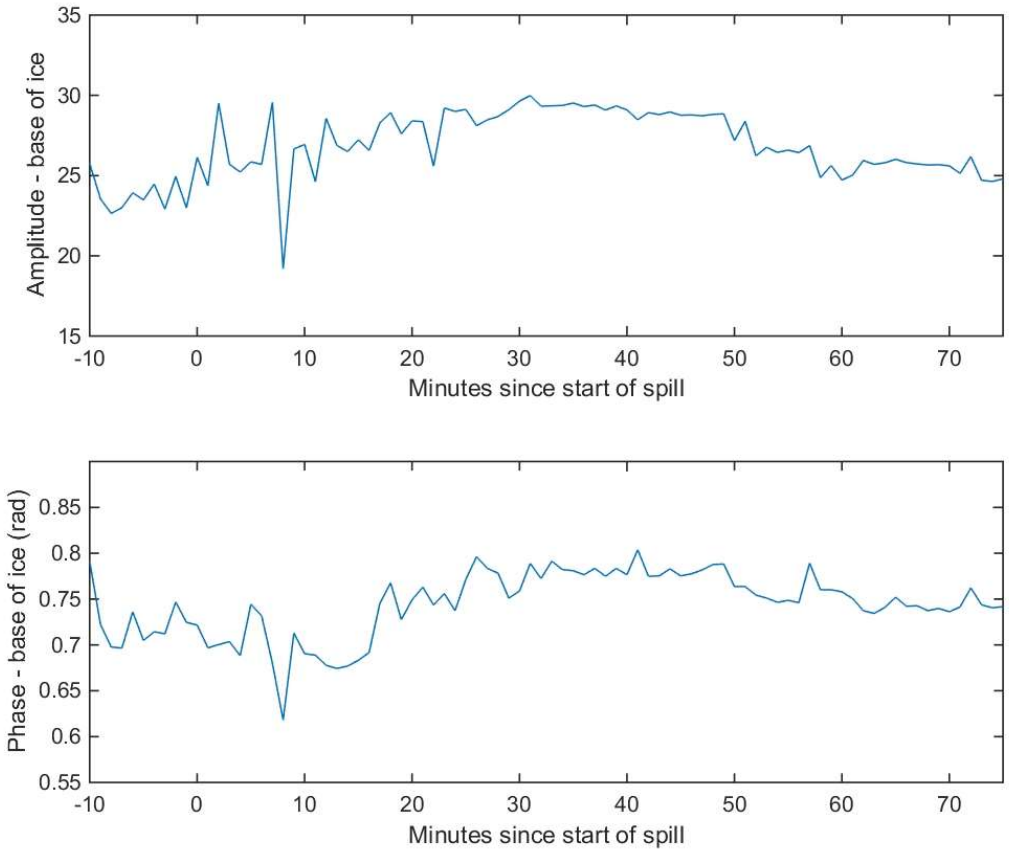

Figure 13 Amplitude and phase of the base of ice reflection.

The amplitude reaches a maximum that is 30% greater than the pre-spill value, 30 minutes after the start of the injection. A small, systematic phase rotation is also observed during this time.

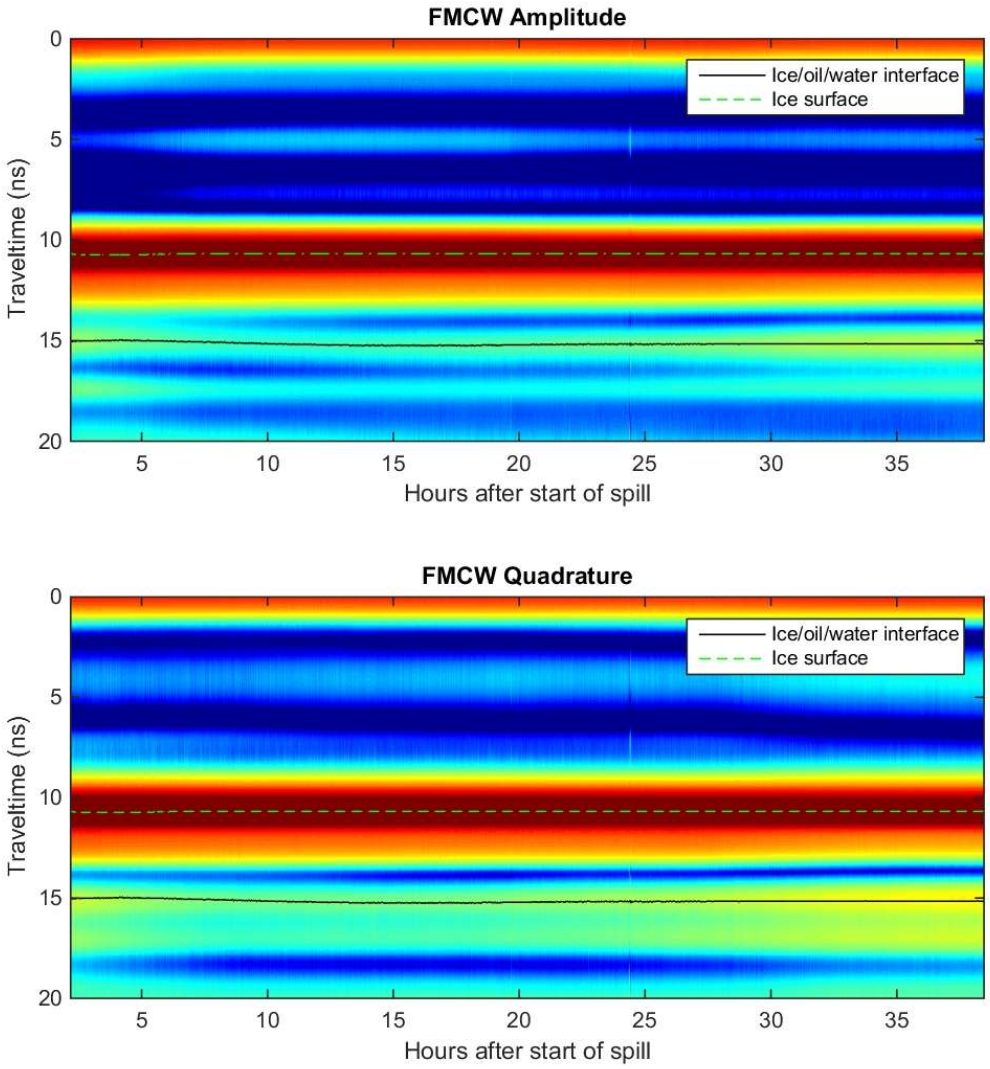

Figure 14 FMCW radar response from 2 hrs to 38 hrs after the start of the spill.

The ice surface reflection remains stable and nearly constant while the base of ice reflection undergoes gradual amplitude changes and peak broadening associated with growth 4 cm of encapsulating ice beneath the oil.

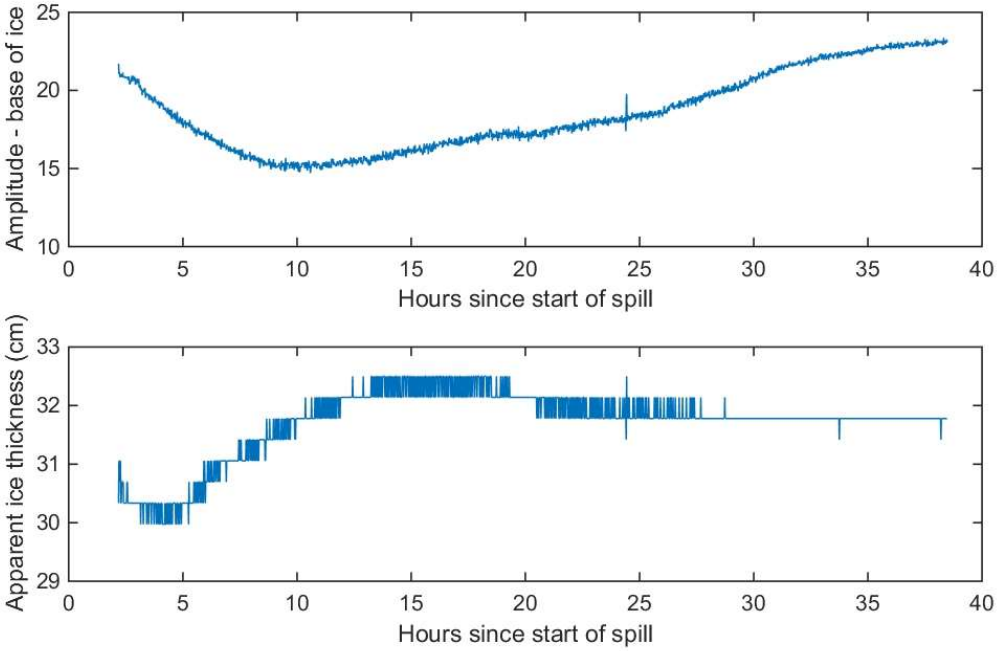

Figure 15 Systematic amplitude variability and increase in the apparent ice thickness are associated with growth of 4 cm of ice beneath the oil during the 38 hrs after the spill.

The apparent depth increase does not indicate the true change of 4 cm because the oil and encapsulating ice layers are not well resolved.

4 MODELING RESULTS

The FMCW radar model used in previous phases of this project was used to simulate radar response during this test. Inputs required for the model are ice salinity and temperature vs depth. Temperature profiles at the time of acquisition (Figure 5) were coupled with salinity measurements made from ice cores at the end of the experiment (Figure 4). The salinity profile was compressed to account for decreased ice thickness at the time of acquisition. Four experiment times were simulated for comparison to the field data – just before the injection, at maximum injected volume 30 minutes after injection began, after the ice temperature profile had recovered 2hrs after injection, and after 38 hrs of encapsulating ice growth (Figure 16). The model was calibrated for field measurements by adjusting the model spectrum to match the pre-injection field signal. This required narrowing the system bandwidth to 850 MHz and increasing the amplitudes at the low end of the spectrum. This resulted in a significant reduction in resolution from the theoretical value, but provides a good comparison to the field data.

The model predicts an increase in amplitude of around 20% as the oil reaches maximum thickness of 5 cm. This is similar to the 30% that was observed in the field data. The model predicts a further increase in amplitude as the ice temperature profile cooled to the values prior to opening the bay doors. This occurs because there is less attenuation in the upper layers of the cooler ice sheet. This effect was not observed in the basin data, and in fact the amplitude decreased during this time. We attribute this divergence between model and basin data primarily to the oil interface becoming diffuse as oil rapidly migrated upward into open brine channels. After 38 hrs, the model predicts broadening of the reflection peak as the composite interface grows in thickness with the encapsulating ice layer. The model predicts an apparent change in total ice thickness of 2 cm over this time. This is consistent with the observed field data.

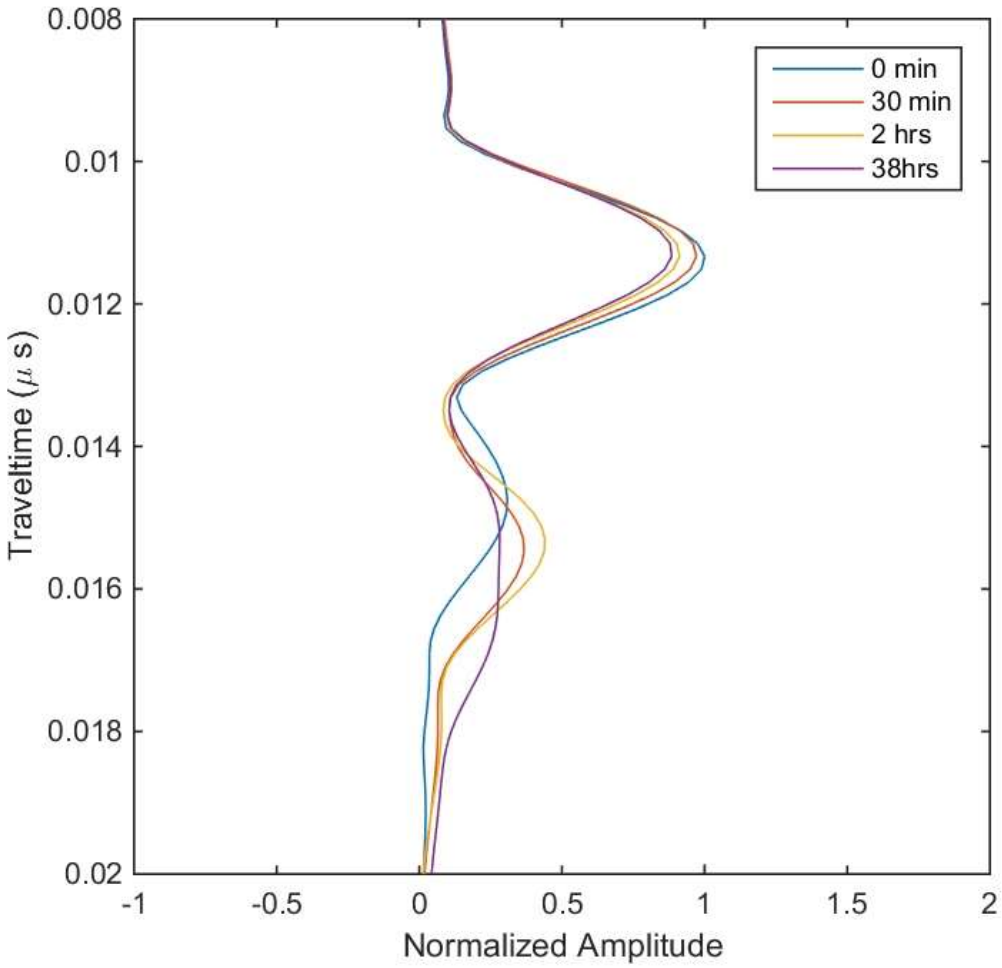

Figure 16 Results of FMCW model simulations at 4 different times during the experiment – just before oil injection, at maximum volume injection (30 min), after the temperature profile had recovered (2hr) and after 38 hrs of encapsulation.

The ice surface reflection is peaked at 11.5 ns and the base of ice peak occurs between 14 and 16 ns.

5 CONCLUSIONS AND RECOMMENDATIONS FOR FUTURE WORK

This basin trial represents the first confirmed detection of oil under ice using the P3 FMCW radar and is a significant advance in the oil under ice detection project. The maximum amplitude increase of 30% with an oil layer thickness of 5 cm is comparable to modeling results. Additionally, the radar response to an oil layer thickness range between 0 and 5 cm was observed as a systematic increase in radar reflection amplitude over ~ 30 minutes required to complete the injection.

Some challenges remain. The surface coupled pulsed radar data remain easier to interpret and produce a stronger response when oil is present beneath the ice. This appears to be primarily due to lowering of the effective resolution of the FMCW system.

Robustness of the radar system was improved dramatically over the project period. However, sensitivities to temperature fluctuations, and to condensation buildup were observed. These latter two issues may not be problematic under field conditions where temperatures are not likely to vary by the ~45 C change observed during this test, nor is there likely to be condensation buildup in arctic conditions.

Recommendations for future work include:

- Continue to improve radar electronics
    - Future work should be focused toward maximizing radar bandwidth to achieve performance closer to the theoretical value
    - Building a fully self-contained, field robust system that includes antennas, control electronics and power source in a single portable package
    - Add truly polarimetric acquisition capability for orthogonal and cross-pole measurements. Such a system may leverage recent developments in multi-channel radar acquisition
- A field test in the Arctic
    - Experience has shown that it is exceptionally difficult to mimic Arctic conditions in a test basin. This and previous tests show that when the radar signal can reach the target depth, oil layers of less than 5 cm produce a measureable radar response. Thus a test that is focused on simply evaluating natural ice penetration would provide extremely valuable field data without the need for an oil spill.
    - The field test should include evaluation from various heights above the ice. This could be done from a crane, but would ideally carried out from a moving platform such as a helicopter. Given the expense of performing any field test in the Arctic, the marginal added cost of a few hours helicopter time would be a worthwhile investment.

6 REFERENCES

Dickins, D.F. 2004. Advancing Oil Spill Response in Ice Covered Areas. Report submitted to the Prince William Sound Oil Spill Recovery Institute and US Arctic Research Commission, Cordova Alaska and Washington DC.

Dickins, D., Liberty L., Hirst W., Bradford J., Jones V., Zabilansky L., G. Gibson G., and J. Lane. 2005. New and Innovative Equipment and Technologies for the Remote Sensing and Surveillance of Oil in and Under Ice. Proceedings 28 th Arctic and Marine Oilspill Program Technical Seminar, Calgary, June 2005. (MMS Contract 1435-01-04-36285)

Dickins, D.F., Buist, I.A., and W.M. Pistruzak. 1981. Dome Petroleum's Study of Oil and Gas Under Sea Ice. Proceedings International Oil Spill Conference, American Petroleum Institute, Wash. D.C., pp 183-189. (Full report in 2 Vols. cited in text as Dickins and Buist, 1981)

NORCOR Engineering and Research Ltd. 1975. The Interaction of Crude Oil with Arctic Sea Ice. Beaufort Sea Project Technical Report No. 27, Canada Department of the Environment, Victoria, British Columbia.

APPENDIX A DETAILS OF RADAR ELECTRONICS MODIFICATIONS

Add 100 nF cap in parallel with parallel with C78 on RF Board

Put feedback network between input and output of PHA1 to eliminate instability at around 50 MHz
Network is a series 47 nH, 100 nF, and 510 ohm resistor

Pick up signal for PLL synthesizer from the output of the filter following the PHA1 gain block with a series 51 ohm resistor to the coax.

Add 510 ohm resistor from output of filter before PHA1 to ground. This eliminates instability at around 3.6 GHz.

Change R16 on unit 1 shaping board from 1k to 1.2k. This shifts output lower on VT1 so that the cp voltage does not bottom out at 0 volts. Unit 2 the value was changed to 3.0k. Note that the shaping board resistor values are different on the two units. See Dropbox/FMCW/Proto3/PCB/Analog/PllLinearizationPNPver1.asc and PllLinearizationPNPver2.asc for actual values.

On RF board change C41, C42, C43, C44 from 33 nF to 100 nF. Change C76 and C77 from 33 nF to 1 uF. This flattens frequency response to reduce effect of higher frequency and harmonic response.